Published in final edited form as:

Catheter Cardiovasc Interv. 2019 February 01; 93(2): 278–285. doi:10.1002/ccd.27726.

Fracture in Drug-Eluting Stents Increases Focal Intimal Hyperplasia in the Atherosclerosed Rabbit Iliac Artery

Claire Conway, PhD[1,*], **Gerard J. Desany, BS**[2], **Lynn R. Bailey, BS**[3], **John H. Keating, DVM DACVP**[3], **Brian L. Baker, MS PE**[2], and **Elazer R. Edelman, MD PhD**[1,4]

[1]Institute for Medical Engineering and Science, Massachusetts Institute of Technology, Cambridge, MA, USA

[2]Winchester Engineering and Analytical Center, US Food and Drug Administration, Winchester, MA, USA

[3]Concord Biomedical Sciences & Emerging Technologies, Lexington, MA USA

[4]Cardiovascular Division, Brigham and Women's Hospital, Harvard Medical School, Boston, MA, USA

Abstract

Objectives—Drug-eluting stent (DES) strut fracture (SF) is associated with higher incidence of In-stent restenosis (ISR) – return of blockage in a diseased artery post stenting – than seen with bare metal stents (BMS). We hypothesize that concomitance of drug and SF leads to greater neointimal response.

Background—Controlled release of therapeutic agents, such as sirolimus and its analogs, or paclitaxel from has reduced tissue based DES failure modes compared to BMS. ISR is dramatically reduced and yet the implications of mechanical device failure is magnified.

Methods—Bilateral Xience Everolimus-eluting stents (EES) were implanted in 20 New Zealand White rabbits on normal (n=7) or high fat/high cholesterol (n=13) diets. Implanted stents were intact or mechanically fractured. Everolimus concentration was as packaged or pre-eluted. After 21 days, stented vessels were explanted, resin embedded, MicroCT scanned, and analyzed histomorphometrically.

Results—Fractured EES were associated with significant ($p < 0.05$) increases in arterial stenosis and neointimal formation and lower lumen-to-artery area ratios compared to intact EES. Hyperlipidemic animals receiving pre-eluted EES revealed no significant difference between intact and fracture groups.

Conclusions—SF increases intimal hyperplasia, post EES implant, and worse with more advanced disease. Pre-eluted groups, reflective of BMS, did not show significant differences, suggesting a synergistic effect of everolimus and mechanical injury, potentially explaining the lack

Address for correspondence: Claire Conway, 77 Massachusetts Ave, Cambridge, MA 02139, USA, Tel: 617-258-8893, Fax: 617-253-2514, cconway@mit.edu.

Conflicts of interest

The authors have no conflicts of interest to report.

of SF reports for BMS. Here we report that ISR has a higher incidence with SF in EES, the clinical implication is that patients with SF after DES implantation merit careful follow-up.

Key terms

Drug-Eluting Stents; Everolimus; Stent Strut Fracture; Pre-Clinical Model

Introduction

In the United States alone, an estimated 92 million adults (more than 1 in 3) suffer from a form of cardiovascular disease (CVD) - with coronary heart disease representing nearly half of all deaths attributed to CVD [1]. The advent of endovascular stenting has revolutionized the treatment of CVD and while immensely impactful the first generation bare metal stents (BMS) were hampered by issues of in-stent-restenosis (ISR), tissue growth over the stent and within the lumen that restricted flow. Some 40% of patients required re-intervention [2]. The development of drug-eluting stents (DES) significantly reduced adverse events by locally eluting high concentrations of anti-proliferative drugs in the vicinity of the stent struts [3].

However, clinical reports of stent strut fracture (SF) in DES emerged soon after clinical introduction [4–6]. Individual case studies described asymptomatic patients with ISR at angiographic follow-up (typically performed after 6 months). Intravascular ultrasound (IVUS) imaging confirmed discontinuity in device integrity and presence of strut fracture. Associated clinical characteristics and implications of SF identified at meta-analysis included longer stents, tortuous vessels, right coronary artery implantations, saphenous venous bypass graft implantations, balloon over-expansion, and overlapping stent configurations. Of the eight included studies for analysis, the mean SF per patient was 4% and ISR increased in the presence of SF. [7]

Nakazawa *et al.* [8] discovered that 29% of stents had a fracture at autopsy, and that 67% of patients with SF suffered an adverse events including in-stent-thrombosis (IST) or ISR. The higher detection rate of SF than reported in clinical observational studies was attributed to the use of a high contrast film-based radiography which is higher resolution (~80 μm) than angiography (~300 μm) or IVUS (~200 μm).

When observed, such SF associated responses are typically reported for DES not BMS. In the present study, we hypothesize that the presence of drug and SF leads to greater neointimal tissue formation, as a precursor to ISR. This hypothesis was tested in a preclinical model of iliac artery atherosclerosis, providing a level of translation that is not possible with bench-top experimental and computational models.

Materials and Methods

Animal systems

Experiments were conducted in male New Zealand White rabbits (Charles River Labs) under a protocol approved by the Institutional Animal Care and Use Committee (IACUC) and conducted according to the United States' Animal Welfare Act and Animal Welfare

Regulations code. Animals were quarantined for a minimum of seven days prior to study initiation and thereafter maintained on controlled diets. Seven rabbits were fed normal chow (Purina Lab Diet High Fiber #5326) and 14 were placed on an atherogenic diet consisting of 0.5% cholesterol and 10% peanut oil for 21 days prior to implantation. This high fat/high cholesterol (HF/HC) group continued on the atherogenic diet for the remainder of the study (Figure 1). In brief, group one (grey) represents fractured DES implanted in a HF/HC model, group two (white) represents intact DES implanted in a HF/HC model, group three (red) represents fractured pre-eluted DES (*pseudo* BMS) in a HF/HC model, group four (green) represents intact pre-eluted DES implanted in a HF/HC model, group five (yellow) represents fractured DES implanted in a healthy model and group six (blue) represents intact DES implanted in a healthy model.

Stent Preparation and Implantation

Animals received clinically ubiquitous 3 × 18 mm Xience (Abbott Vascular; Santa Clara, CA) Everolimus eluting stents (EES) in each of their iliac arteries, assigned randomly to alternate between an intact stent or one with mechanically cut strut fractures. To promote uniformity of handling each device was balloon inflated, placed on a mandrel (see Figure 2), kept intact or mechanically cut, then removed from mandrel and re-crimped onto balloon catheter assembly. Locations of mechanical cuts were assigned to regions of predicted failure from our previous computational study [9]. These mechanical cuts resulted in devices with grade II fractures, as per Carter scheme [10]. A subset of drug-eluting stents (n=14) were soaked for five minutes in Dimethyl Sulphoxide (DMSO) and then triple washed in sterile saline, to represent an eluted time-point for the device prior to recrimping, representing a *pseudo* BMS device grouping. This grouping justification was two-fold; firstly to represent a device without drug present (*pseudo* BMS) and secondly to represent a polymer-coated DES at a timepoint when all drug has been eluted – capturing a realistic DES porous surface. Pharmacokinetic analysis by high-performance liquid chromatography of one stent sample confirmed complete elution of the drug after soaking in DMSO. The definition of stent and animal groups is illustrated in Figure 1. All handling of devices was performed aseptically in the sterile operating room.

Animals received Ketamine (25–35 mg/kg) and Xylazine (1–5 mg/kg) combined injection administered subcutaneously for induction of anesthesia. Once chemically immobilized, the animals were intubated and maintained on continuous isoflurane inhalant anesthesia delivered to effect in 100% oxygen for the remainder of the procedure. Pre-emptive analgesia, buprenorphine (0.01 mg/kg, subcutaneous), was administered at time of anesthesia induction (prior to surgical incision). Under fluoroscopic guidance, an angiographic catheter was advanced, via carotid artery incision, to the iliac arteries. Angiographic images with contrast identified deployment sites. Each device was introduced by advancing the stent delivery system over the guide catheter and guide wire to the deployment site. Balloons were inflated at a steady rate to deploy each device and complete balloon deflation was verified with fluoroscopy.

Total Plasma Cholesterol

Blood samples were collected from a peripheral vessel at 21 days prior to implant (HF/HC diet initiation), day 0 (stent implantation) and 21 (prior to necropsy) (see Figure 1). These samples were collected to monitor and assess the animal's health during the study and prior to euthanization. Animal body weights, with a body condition score, were recorded at days 0, 7, 14, and 21.

Stent Harvest and Preparation

Animal were euthanized 21 days after stent implantation via an IV overdose of euthanasia solution in accordance with American Veterinary Medical Association guidelines [11]. Stented arteries were harvested for histopathological examination. Each artery was perfused at ~ 100 mmHg with a physiologic solution followed by 10% Neutral Buffer Formaldehyde (NBF). The stented arteries were removed *en bloc* and placed in 10% NBF filled containers to ensure vessel integrity prior to processing, embedding, sectioning and histopathologic analysis.

Radiography and MicroCT

Two approximately perpendicular radiographs were taken to document stent location and morphology *in situ*. Following necropsy, additional radiographs were obtained to assist in assessment of expanded stent morphology, damage and/or strut fracture sites. Post-embedding of the stented arteries in resin, microCT was performed on each sample (GE eXplore CT 120, 50 micron resolution; Little Chalfont, UK). The microCT scans, in DICOM format, were viewed and segmented for isolation of each stent specimen and then converted to a sold representation (SCANIP v7; Simpleware, UK). Following 3D reconstruction, each specimen was inspected for fracture or discontinuities (Figure 3). Particular attention was paid to the pre-fracture site locations in order to verify successful micro-cutting of the stent struts.

Light Microscopy and Histomorphometry

Resin embedded specimens were sectioned transversely in three regions. For intact stents, transverse sections were obtained from the proximal, mid and distal regions. For pre-fractured stents, transverse sections of the stented vessel portion were obtained from the proximal, mid and distal region targeting areas stent strut fracture, as previously determined by micro-CT. All vessel sections were stained by hematoxylin-eosin (H&E) and Verhoeff's tissue elastin stain.

Quantitative histomorphometric analysis was performed on each stented artery. Histological sections were measured using computer-assist software (Olympus cellSens Dimension Desktop, v1; Olympus, Hamburg, Germany). Area measurements included the neointima, internal elastic lamina bounds, stent, and artery to external elastic lamina bounds. Stented segments were also histomorphologically scored for parameters such as injury, inflammation, endothelialization, neointimal fibrin deposition, and adventitial fibrosis.

Statistical Analysis

All histological data scores were reported as the group mean ± SD. Data sets were assessed for normality and variance equivalence. When these conditions were met a t-test was conducted; otherwise a Mann-Whitney rank sum test was conducted. A $P<0.05$ was considered statistically significant. All statistics were calculated with SigmaPlot version 11 (Systat Software Inc.; San Jose, CA) software.

Results

Animal Condition and Cholesterol Levels

At the conclusion of the study, 39 stents (n=13 each of fractured EES and intact EES, n=7 of fractured pre-eluted stents and n=6 of intact pre-eluted stents) were successfully harvested from 20 animals that appeared to be in good health. One animal intended for study was excluded prior to stent placement because of evident aortic thrombus and one fractured pre-eluted stent was stripped from the delivery system in the introducer sheath and could not be implanted. Animals on standard chow had clear serum and cholesterol levels within normal range - mean levels of circulating cholesterol at baseline were 51 ± 24 mg/dL, at implant were 32 ± 7 mg/dL and at pre-necropsy were 27 ± 13 mg/dL. Animals on the HFHC diet (n=13) had elevated levels of serum at the time of implant and before necropsy. The HFHC groups' serums appeared cloudy/fatty, confirming hyperlipidemia. In the HFHC group, the mean levels of circulating cholesterol at baseline (prior to HFHC diet initiation) were 45 ± 21 mg/dL, at implant rose 25-fold to 1155 ± 374 mg/dL and at pre-necropsy even further to 1553 ± 325 mg/dL.

MicroCT and Radiography

All pre-fracture locations in the fractured specimen groups were identified during 3D reconstruction of microCT DICOM images (see Figure 3 for fracture verification example). No additional fractures were noted in any group, intact or pre-fractured. The comparison with radiographs was performed as an additional qualitative check. Not all fractures could be identified in radiographs, due to the limited number of views captured.

Morphometric and Histological Evaluation

Following intact EES implantation when animals were maintained on a HF/HC diet (comparing groups 2 and 6 – Table I), there was elevated arterial stenosis (by 3%), neointimal area (by 0.12 mm^2), and neointimal thickness (by 0.02 mm) and reduced lumen area to artery area (by 0.03) in (Figure 4 and Table I). Removal of drug from intact stents via pre-elution (comparing groups 2 and 4) and increased these effects by 2%, 0.11 mm^2, 0.02 mm, and reduced by 0.02 respectively. Introduction of SF in EES induced even greater and statistically significant changes ($p < 0.05$) in both HF/HC (comparing groups 1 and 2) by 5%, 0.27 mm^2, 0.04 mm, and 0.05. Similarly, introduction of SF in EES in animals on normal diets (comparing groups 5 and 6) induced statistically significant changes by almost identical values of 5%, 0.26 mm^2, 0.04 mm, and 0.05. Interestingly, when SF was induced in pre-eluted EES no statistical differences were observed. Those statistically significant

morphological differences are further illustrated in Figure 5 as a visual guide for group comparison.

In all groups injury was minimal, endothelialization was complete or nearly complete, neointima was mature and consisted of organized smooth muscle cells, and adventitial fibrosis was absent (Supplementary Tables A-I and A-II). However, two parameters, inflammation and neointimal fibrin, showed differences in HF/HC groups. Inflammation in the normolipidemic groups was comparable. The presence of fracture in the hyperlipidemic groups induced higher inflammation compared to intact equivalents. Neointimal fibrin was minimal or absent in pre-eluted groups, but when drug and fracture were present neointimal fibrin increased, particularly in disease (Supplementary Table A-III provides detailed statistical summary).

It was also noted that foam cells (lipid filled macrophages which are a key atheroma constituent) were only present in hyperlipidemic groups. Neointimal foam cell scores and frequency were highest in hyperlipidemic animals with pre-eluted stents, through scores overall were minimal.

Discussion

Despite clinical reports of SF in DES and associated increased risk of ISR, it has not been established whether SF is the cause of the increased neointimal response. Here we demonstrate that while drug and SF are present the patient is at potentially greater risk of ISR. This study illustrates, using precise control of presence of drug, SF, and disease state, how these factors combine to generate a greater neointimal response.

In the present study, in examining the confluence of factors that affect the vascular response to EES implantation we can now align the response in animals to that seen in humans and further explain clinical observations[7,8,12,13]. Mechanical, inflammatory and metabolic effects come together with SF and dietary manipulation and when all are preset vascular injury is maximized and repair least effective. Fracture in EES exacerbates formation of neointimal tissue, especially in conjunction with HF/HC diet. While the intent of the therapeutic drug in EES is to reduce anti-proliferative effects, it can delay endothelialization and in the presence of SF, drug may enhance vessel injury and subsequent inflammatory response, as seen in from the results of this work.

To reinforce this point, in the HF/HC groups of pre-eluted DES (or *pseudo* BMS) these significant differences in neointimal measurements of thickness and area are not observed. This points to the key role that drug and SF have in exacerbating vascular response in the form of neointimal formation.

There are distinct advantages and disadvantages of animal models in examining interventional procedures [14]. Arterial repair follows a similar coordinated sequence of biological events involved in vascular healing in both man and animal, though more rapidly and more repeatably in the latter [15]. The rabbit iliofemoral model exhibits less of an inflammatory foreign body reaction and slower rates of endothelial strut coverage (compared to the swine coronary model often selected in stent safety studies), although the latter

process is still accelerated relative to human response [16]. The 21 day duration was determined to be suitable as a similar study demonstrated nearly 100% endothelialization at 21 days with similar devices [17]. In addition, the acceleration of an atherosclerotic disease state on high fat diet and the size of the iliac artery being similar to human coronary arteries made this an attractive model system. Given the reproducibility of the rabbit [14,18–20] and lack of a reliable atherosclerotic porcine model [21], despite the potential disadvantages, the selection of this iliofemoral model was deemed appropriate.

In terms of justification for the choice of pre-eluted EES as a *pseudo BMS*, it has been shown that angiographic and histological results in a porcine coronary model that polymer-coated stents were equivalent to the bare-metal version of device at 28, 90 and 180 day timepoints [22]. In addition any inflammation (negligible to mild) with polymer-coated devices paralleled that of the bare-metal equivalent in this study.

It should also be noted that study findings were enhanced by advanced technical processes. To ensure that each fracture site was successfully cut, microCT of the explanted stented vessels was performed (see Figure 3). The verification of fracture at each of the six pre-fracture sites per device ensured that the observed results could be directly linked to presence of stent strut fracture. The representative histological images (Figure 4) illustrate what is confirmed with histomorphometric measurements (Table I and Figure 5); that there is greater neointimal tissue formation in the presence of fracture compared to intact devices when drug is present, both in healthy and diseased animals. As a result of neointimal tissue growth, lumen area to artery area ratio is also significantly reduced in the presence of SF.

Placing these results in context, Perkins et al. [22] evaluated the everolimus-release profile of the Xience EES in a porcine coronary artery model and found that after 28 days ~ 71% of everolimus was released from the device and that everolimus concentration in the stented arterial vessel was 0.8 ng/mg at this timepoint. Relating these results to our 21 day study leads to the conclusion that everolimus is still expected to be present in the device and surrounding iliac tissue. Based on our data, showing the increased neointimal hyperplasia response in EES with SF present, there is a detrimental effect of the therapeutic agent when fracture is present.

This leads to the concern that SF while drug is present (95% of everolimus is released at four months [22]) can lead to increased neointimal response. Interestingly, case studies reporting SF [4–6,23] with ISR formation have been five to eight months post device implant. This means SF could have occurred at any stage prior to follow-up investigation i.e. drug may still have been present resulting in this adverse outcome of ISR.

This study points to the need for rigorous examination of patients at follow-up for evidence of device discontinuity or SF, particularly in the case of DES implants. Often occurring at sites of inconsistent motion such as ‘hingepoints’ this can be a difficult to detect through angiographic means alone. When predisposing factors are present, as reviewed in Chakarvarty *et al.* [7], such as longer stents, vessel tortuosity, right coronary artery location, overlapping configurations and devices over-expanded at implant, the examination at follow-up should be potentially be at an earlier timepoint, while drug elution is likely still

occurring, and examination needs to be even more considerate. Though patients may present as asymptomatic the evidence in this study suggests they are at a potentially greater risk of ISR and merit particular attention and observation.

Summary and Perspective

DES interventions are still hampered by issues of ISR. With this generation of device, if SF occurs this has been linked to higher rates of ISR formation. This study examines the consequence of controlled SF in a rabbit iliac model of atherosclerosis after 21 days. The results indicate that, in the presence of SF in DES there is a significantly greater formation of neointimal area and also significantly reduced lumen area to artery area ratios. Pre-eluted stents, which are intended to be reflective of BMS, did not show significant differences between intact and fracture state. This potentially explains the lack of clinical SF reports for BMS.

This study provides insight into why SF with DES results in higher incidence of ISR. Patients detected with SF after receiving DES need careful examination and follow-up (even if asymptomatic); as this study has taken steps towards demonstrating that ISR has a higher incidence in the presence of SF and DES.

Supplementary Material

Refer to Web version on PubMed Central for supplementary material.

Acknowledgments

This work was funded in part by a grant, R01 GM49039 (ERE), from the National Institute of Health and appointment to the Research Participation Program at FDA administered by Oak Ridge Institute for Science and Education (CC).

References

1. Benjamin EJ, Blaha MJ, Chiuve SE, Cushman M, Das SR, Deo R, et al. Heart Disease and Stroke Statistics—2017 Update: A Report From the American Heart Association. Circulation. 2017; 135:e146–e603. [PubMed: 28122885]
2. Bainey KR, Norris CM, Graham MM, Ghali WA, Knudtson ML, Welsh RC. Clinical in-stent restenosis with bare metal stents: Is it truly a benign phenomenon? Int J Cardiol. 2008; 128:378–382. [PubMed: 17689711]
3. Morice M-C, Serruys PW, Sousa JE, Fajadet J, Ban Hayashi E, Perin M, et al. A Randomized Comparison of a Sirolimus-Eluting Stent with a Standard Stent for Coronary Revascularization. N Engl J Med. 2002; 346:1773–1780. [PubMed: 12050336]
4. Sianos G, Hofma S, Ligthart JMR, Saia F, Hoye A, Lemos PA, et al. Stent fracture and restenosis in the drug-eluting stent era. Catheter Cardiovasc Interv. 2004; 61:111–116. [PubMed: 14696169]
5. Halkin A, Carlier S, Leon MB. Late incomplete lesion coverage following Cypher stent deployment for diffuse right coronary artery stenosis. Heart Br Card Soc. 2004; 90:e45.
6. Min P-K, Yoon Y-W, Moon Kwon H. Delayed strut fracture of sirolimus-eluting stent: a significant problem or an occasional observation? Int J Cardiol. 2006; 106:404–406. [PubMed: 16337054]
7. Chakravarty T, White AJ, Buch M, Naik H, Doctor N, Schapira J, et al. Meta-Analysis of Incidence, Clinical Characteristics and Implications of Stent Fracture. Am J Cardiol. 2010; 106:1075–1080. [PubMed: 20920641]

8. Nakazawa G, Finn AV, Vorpahl M, Ladich E, Kutys R, Balazs I, et al. Incidence and Predictors of Drug-Eluting Stent Fracture in Human Coronary ArteryA Pathologic Analysis. J Am Coll Cardiol. 2009; 54:1924–1931. [PubMed: 19909872]
9. Everett KD, Conway C, Desany GJ, Baker BL, Choi G, Taylor CA, et al. Structural Mechanics Predictions Relating to Clinical Coronary Stent Fracture in a 5 Year Period in FDA MAUDE Database. Ann Biomed Eng. 2016; 44:391–403. [PubMed: 26467552]
10. Carter AJ. Stent strut fracture: Seeing is believing. Catheter Cardiovasc Interv. 2008; 71:619–620. [PubMed: 18360854]
11. American Veterinary Medical Association. [cited 2016 Sep 23] Guidelines for the Euthanasia of Animals: 2013 Edition. 2013. Available from: https://www.avma.org/KB/Policies/Documents/euthanasia.pdf
12. Shaikh F, Maddikunta R, Djelmami-Hani M, Solis J, Allaqaband S, Bajwa T. Stent fracture, an incidental finding or a significant marker of clinical in-stent restenosis? Catheter Cardiovasc Interv. 2008; 71:614–618. [PubMed: 18360853]
13. Yang T-H, Kim D-I, Park S-G, Seo J-S, Cho H-J, Seol S-H, et al. Clinical characteristics of stent fracture after sirolimus-eluting stent implantation. Int J Cardiol. 2009; 131:212–216. [PubMed: 18241940]
14. Nakazawa G, Nakano M, Otsuka F, Wilcox JN, Melder R, Pruitt S, et al. Evaluation of Polymer-Based Comparator Drug-Eluting Stents Using a Rabbit Model of Iliac Artery Atherosclerosis. Circ Cardiovasc Interv. 2011; 4:38–46. [PubMed: 21205943]
15. Virmani R, Kolodgie FD, Farb A, Lafont A. Drug eluting stents: are human and animal studies comparable? Heart. 2003; 89:133–138. [PubMed: 12527658]
16. Finn AV, Nakazawa G, Joner M, Kolodgie FD, Mont EK, Gold HK, et al. Vascular Responses to Drug Eluting Stents. Arterioscler Thromb Vasc Biol. 2007; 27:1500–1510. [PubMed: 17510464]
17. Groothius, A; Seifert, P; Spognardi, AM; Markham, P; Price, S; Edelman, ER. [cited 2017 Oct 2] TCT 2010: A Comprehensive Analysis of DES and Bare Metal Stents Using Morphometric SEM Images of Overlapping Stent Pairs in a Rabbit Iliac Model to Assess Overall HealingCBSET | CBSET. Available from: http://cbset.org/tct-2010-a-comprehensive-analysis-of-des-and-bare-metal-stents-using-morphometric-sem-images-of-overlapping-stent-pairs-in-a-rabbit-iliac-model-to-assess-overall-healing/
18. Abela GS, Picon PD, Friedl SE, Gebara OC, Miyamoto A, Federman M, et al. Triggering of Plaque Disruption and Arterial Thrombosis in an Atherosclerotic Rabbit Model. Circulation. 1995; 91:776–784. [PubMed: 7828306]
19. Faxon DP, Sanborn TA, Weber VJ, Haudenschild C, Gottsman SB, McGovern WA, et al. Restenosis following transluminal angioplasty in experimental atherosclerosis. Arterioscler Thromb Vasc Biol. 1984; 4:189–195.
20. Danenberg HD, Golomb G, Groothuis A, Gao J, Epstein H, Swaminathan RV, et al. Liposomal Alendronate Inhibits Systemic Innate Immunity and Reduces In-Stent Neointimal Hyperplasia in Rabbits. Circulation. 2003; 108:2798–2804. [PubMed: 14610008]
21. O'Brien CC, Lopes AC, Kolandaivelu K, Kunio M, Brown J, Kolachalama VB, et al. Vascular Response to Experimental Stent Malapposition and Under-Expansion. Ann Biomed Eng. 2016; 44:2251–2260. [PubMed: 26732391]
22. Perkins LEL, Boeke-Purkis KH, Wang Q, Stringer SK, Coleman LA. XIENCE VTM Everolimus-Eluting Coronary Stent System: A Preclinical Assessment. J Intervent Cardiol. 2009; 22:S28–S40.
23. Hamilos MI, Papafaklis MI, Ligthart JM, Serruys PW, Sianos G. Stent fracture and restenosis of a paclitaxel-eluting stent. Hell J Cardiol. 2005; 46:439–442.

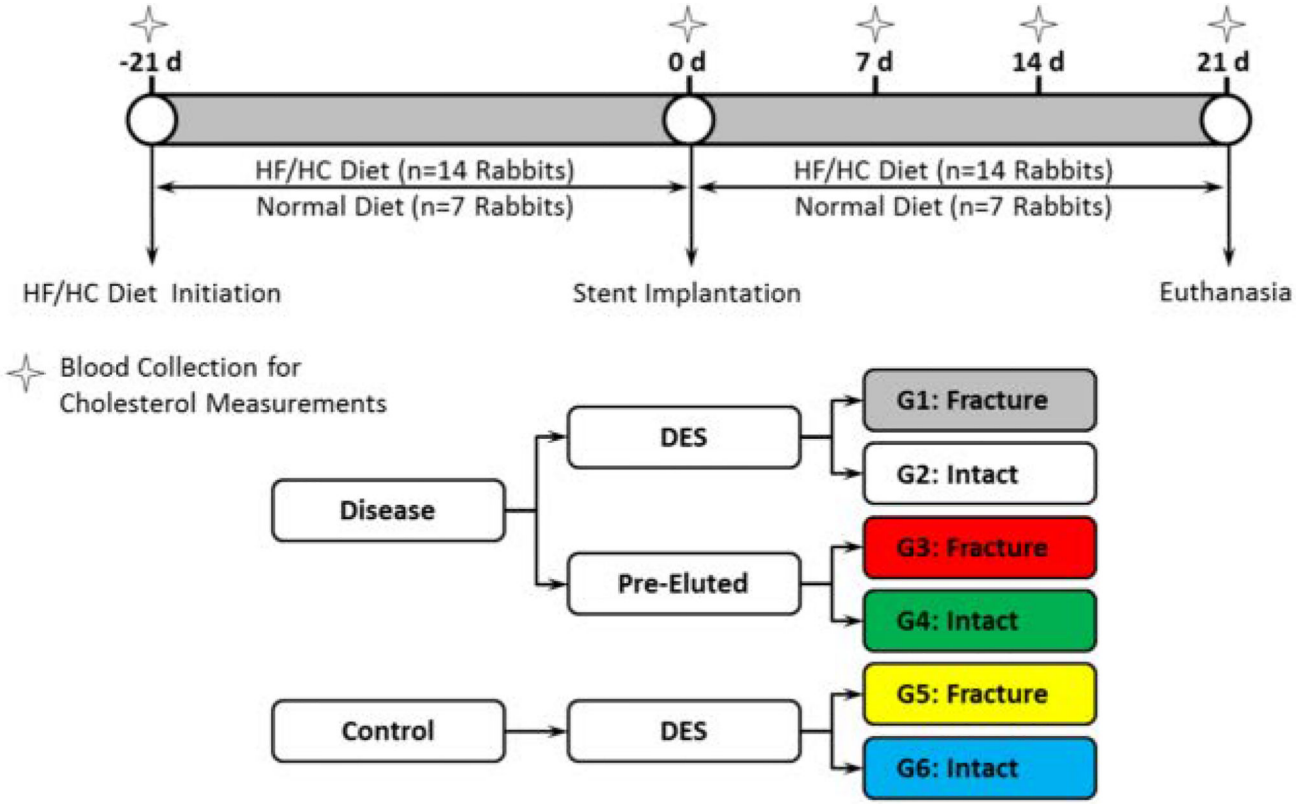

Figure 1.
Study design: timeline and group definition.

Figure 2.
Schematic for fracture locations and equipment for pre-fracturing stent specimens.

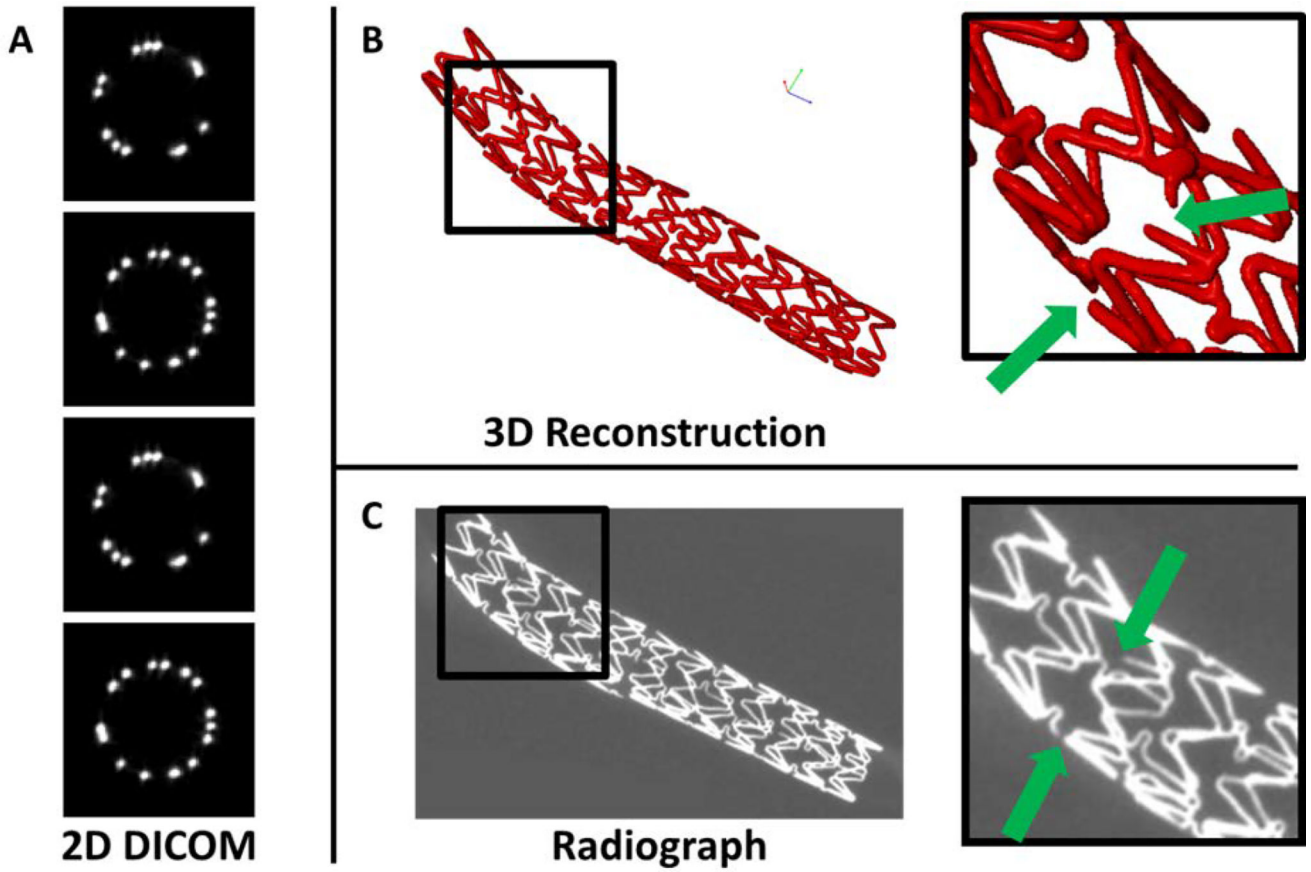

Figure 3.

Fracture site verification. A) Raw 2D DICOM images, B) 3D reconstruction of stent specimen, insert highlighting two pre-fracture locations and C) equivalent radiograph image of stent specimen, insert highlighting the same two pre-fracture locations.

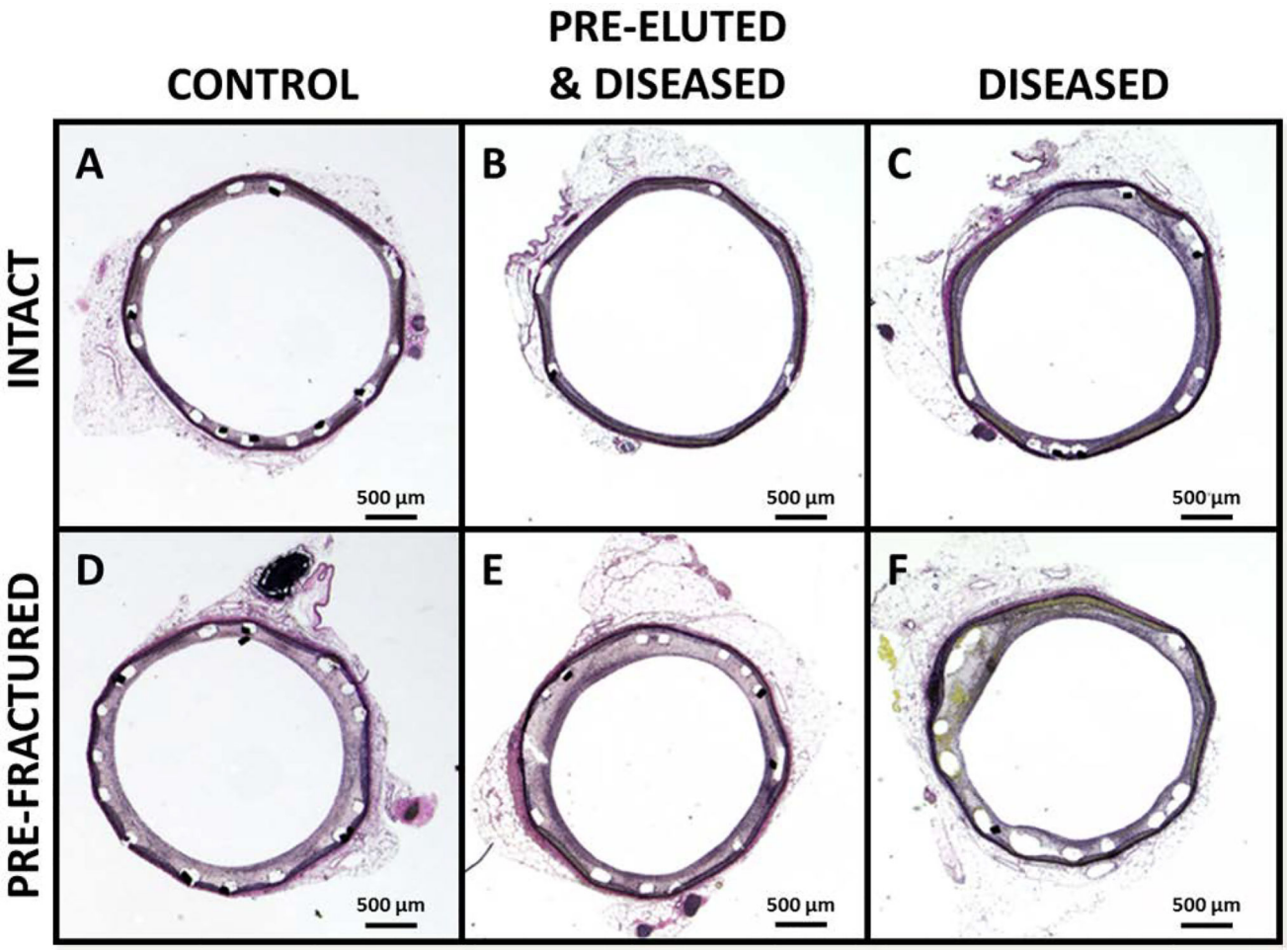

Figure 4.

Histology of representative cross-sections of stented rabbit iliac arteries. A) Healthy control with intact drug-eluting stent (DES), B) High fat high cholesterol (HFHC) “diseased’ model vessel with intact pre-eluted stent, C) HFHC model with intact DES, D) healthy control with pre-fractured DES, E) HFHC model vessel with pre-fractured pre-eluted stent and F) HFHC model with fractured DES. High resolution versions of each panel image (A–F) are available in the Online Supplementary Materials.

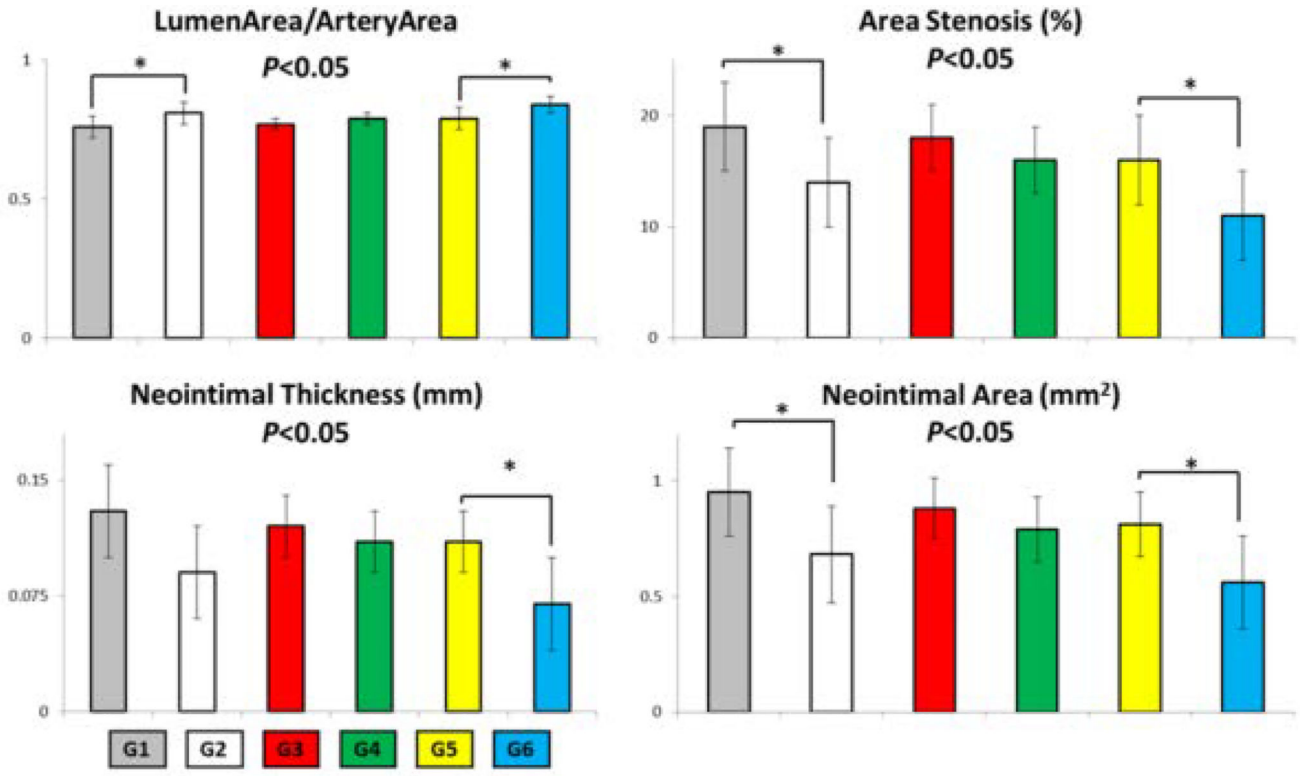

Figure 5.

Bar graphs of morphological parameters in 21 day study of stented rabbit iliac arteries (see Figure 1 for group definition).

Table I

Mean ± SD histomorphometric parameters.

		HF/HC Diet				Normal Diet		
		G1 (n=6)	**G2 (n=6)**	**G3 (n=7)**	**G4 (n=6)**	**G5 (n=7)**	**G6 (n=7)**	***p*****
Area Measurements	Artery Area (mm^2)	5.32 ± 0.38	5.37 ± 0.54	5.36 ± 0.53	5.46 ± 0.53	5.64 ± 0.41	5.80 ± 0.62	0.172
	Medial Area (mm^2)	0.34 ± 0.04	0.37 ± 0.06	0.38 ± 0.06	0.37 ± 0.09	0.39 ± 0.04	0.36 ± 0.06	0.097
	Neointimal Area (mm^2)	0.95 ± 0.19 *	0.68 ± 0.21 *	0.88 ± 0.13	0.79 ± 0.14	0.81 ± 0.14 ‡	0.56 ± 0.2 ‡	<0.05
	Lumen Area (mm^2)	4.03 ± 0.36	4.32 ± 0.53	4.10 ± 0.43	4.30 ± 0.46	4.44 ± 0.49	4.87 ± 0.61	0.116
	Stent Area (mm^2)	5.12 ± 0.38	5.16 ± 0.50	5.17 ± 0.50	5.27 ± 0.49	5.43 ± 0.39	5.57 ± 0.59	0.18
Stenotic Parameters	Neointimal Thickness (mm)	0.13 ± 0.03	0.09 ± 0.03	0.12 ± 0.02	0.11 ± 0.02	0.11 ± 0.02 ‡	0.07 ± 0.03 ‡	<0.05
	Lumen Area / Artery Area	0.76 ± 0.04 §	0.81 ± 0.04 §	0.77 ± 0.02	0.79 ± 0.02	0.79 ± 0.04 †	0.84 ± 0.03 †	<0.05
	Area Stenosis (%)	19 ± 4 *	14 ± 4 *	18 ± 3	16 ± 3	16 ± 4 ‡	11 ± 4 ‡	<0.05

* G1 increased vs. G2 $p < 0.05$

§ G1 decreased vs. G2 $p < 0.05$

‡ G5 increased vs. G6 $p < 0.05$

† G5 decreased vs. G6 $p < 0.05$

G1 = Fractured DES, HF/HC Diet
G2 = Intact DES, HF/HC Diet
G3 = Fractured Pre-Eluted, HF/HC Diet
G4 = Intact Pre-Eluted, HF/HC Diet
G5 = Fractured DES, Normal Diet
G6 = Intact DES, Normal Diet

** Complete statistical summary provided in Table A-III